

CRYSTAL STRUCTURES OF THE HUMITE MINERALS: III.
Mg/Fe ORDERING IN HUMITE AND ITS RELATION TO
OTHER FERROMAGNESIAN SILICATES

P. H. RIBBE AND G. V. GIBBS, *Department of Geological Sciences, Virginia Polytechnic Institute and State University, Blacksburg, Virginia 24061*

ABSTRACT

The crystal structure of humite $[Mg_{6.6}Fe_{0.4}(SiO_4)_3F(OH)]$; a 4.7408(1); b 10.2580(2); c 20.8526(4) Å; $Pbnm$ has been refined to a residual of $R=0.042$. The steric details of the structure are similar to those of norbergite and chondrodite and can be understood in terms of geometrical and electrostatic interactions. In humite there are four distinct octahedra: $M(1)O_6$ and $M(2)O_6$ like those in olivine and $M(2)O_6(F,OH)_1$ and $M(3)O_4(F,OH)_2$ like those in chondrodite.

Ferrous iron is ordered in equal amounts ($\sim 0.1 Fe^{2+}$) into the more distorted octahedra with six oxygen ligands but avoids the less distorted octahedra with one or two (F,OH) ligands. However, in Mg/Fe- containing amphiboles, Fe^{2+} prefers the more distorted $M(3)O_4(OH,F)_2$ and $M(1)O_4(OH,F)_2$ octahedra over the less distorted $M(2)O_6$ octahedron, despite the ligancy. This is rationalized on the basis that the $M(2)$ cation is bonded to two highly electrostatically undersaturated oxygens, which may be less polarizable than OH^- or F^- .

Size criteria fail to predict the Mg/Fe distributions observed in chondrodite and humite. In these close-packed orthosilicates all anions are charge-balanced and Fe^{2+} prefers the more distorted sites and those with the more polarizable ligands. In Mg/Fe olivines the $M(1)O_6$ octahedron is significantly smaller but slightly more distorted than $M(2)O_6$. This may explain the highly disordered Mg/Fe configurations observed in olivines (Brown, 1970) and the slight ordering of Fe^{2+} into $M(1)O_6$ reported by Finger (1970) for terrestrial and lunar olivines.

Considerations of $M-(F,OH)$ bond lengths in tremolite, protoamphibole, and the humite minerals and $F \rightleftharpoons OH$ -related volume changes in topaz give radii of 1.32₅ Å and 1.34 Å, respectively, for two- and three-coordinated OH ions, based on Shannon and Pre-witt's (1969) fluorine radii.

INTRODUCTION

The crystal structures of the humite minerals,



where $n=1$ for norbergite, $n=2$ for chondrodite, $n=3$ for humite, and $n=4$ for clinohumite, and M is Mg, Fe, Mn, Ca, and Zn in decreasing order of abundance, were determined by Bragg and West (1927) and Taylor and West (1928; 1929). Recent refinements of norbergite (Paper I, Gibbs and Ribbe, 1969) and chondrodite (Paper II, Gibbs, Ribbe, and Anderson, 1970) produced precise atomic parameters which have led to an interpretation of these structures in terms of distortions of the ideal hexagonal close-packed anion array caused by cation-cation repulsion across shared polyhedral edges. Initial studies of humite,

$Mg_{6.6}Fe_{0.4}(SiO_4)_3F(OH)$, yielded the first evidence of Mg/Fe ordering in these close-packed orthosilicates (Ribbe and Gibbs, 1969).

In 1950 Borneman-Starynkevich and Myasnikov concluded on the basis of stoichiometric calculations that the replacement of Mg by Fe in the humite minerals takes place in the "olivine portion" of the structure and not in the "(F,OH) portion." It would be difficult to rationalize this conclusion for norbergite, since both the $M(2)_4$ and $M(3)$ octahedral sites are coordinated by four oxygen and two (F,OH) ligands. The "olivine portion" of the formula which can be written $(Mg,Fe)_2SiO_4 \cdot Mg(F,OH)_2$, has no structural significance (Ribbe, Gibbs, and Jones, 1968). For chondrodite the $M(1)$ octahedron is similar to that in olivine, but the $M(2)_5$ and $M(3)$ octahedra have no analogs in olivine. However, in addition to $M(2)_5$ and $M(3)$ octahedra which are like those in chondrodite, humite contains the $M(1)$ and $M(2)_6$ octahedra of olivine which can be interpreted as the "olivine portion" of the structure. In agreement with the prediction of Borneman-Starynkevich and Myasnikov, Ribbe and Gibbs (1969) found that 70 per cent of the Fe^{2+} in humite is ordered into the "olivine-like" sites, $M(1)$ and $M(2)_6$. Chondrodite was subsequently found to have Fe^{2+} ordered into the $M(1)$ octahedron with six oxygen ligands, whereas the $M(2)_5$ octahedron with $O_5(F,OH)_1$ ligands and $M(3)$ with $O_4(F,OH)_2$ ligands contained no iron.

EXPERIMENTAL PROCEDURES

The humite used in this study is from a "limestone" at Sillböle, Finland. It was originally analyzed by Rankama (1938) and later examined by Sahama (1953—his specimen No. 3) and Jones, Ribbe, and Gibbs (1969—their specimen No. 7). Its composition, cell parameters, and physical properties are listed in Table 1. The space group $Pbnm$ is consistent with that determined by Taylor and West (1928) and is the preferred setting for purposes of comparison with olivine and the other humite minerals (Jones, 1969).

More than 650 non-zero intensity data $Ok\bar{l}-4kl$ were recorded on a Weissenberg single-crystal diffractometer. The data were collected, processed and weighted in the same manner as those for chondrodite (see Gibbs *et al.*, 1970). Observed and calculated structure amplitudes and weighting factors are listed in Table 2.¹

The initial least-squares refinement was carried out using ORFLS (Busing *et al.*, 1962) and the atomic coordinates of Taylor and West (1928). The small amount of Mn was included as Fe in the scattering factor curves for the octahedral sites. A disordered distribution of Fe was assumed, and the temperature factors for the $M(1)$ and $M(2)_6$ sites refined to 0.2 and 0.01 \AA^2 , respectively, while those for the $M(2)_5$ and $M(3)$ sites calculated relatively large, 0.7 and 0.9 \AA^2 (see Table 3). This suggested Fe^{2+} ordering in the $M(1)$ and

¹ Table 2 has been deposited with the National Auxiliary Publication Service. To obtain a copy, order NAPS Document No. 01483 from National Auxiliary Publications Service of the A.S.I.S., c/o CCM Information Corporation, 909 Third Avenue, New York, 10022; remitting \$1.00 for microfiche or \$5.00 for photocopies; payable to CCMIC-NAPS, in advance.

TABLE 1. MICROPROBE ANALYSIS AND PHYSICAL PROPERTIES OF HUMITE FROM SILLBÖLE, FINLAND

<i>Microprobe analysis</i> (Jones <i>et al.</i> , 1969)					
SiO ₂	36.43 wt. %	CaO	0.01 wt. %		
FeO	5.03	ZnO	0.00		
MnO	0.65	F	4.07		
MgO	53.84	OH(calc.)	3.20		
TiO ₂	0.10	Total, corrected for F, OH: 100.11 wt. %			
<i>Chemical formula</i> , normalized to three Si:					
Mg _{0.607} Fe _{0.350} Mn _{0.045} Ca _{0.001} (SiO ₄) ₃ · Mg _{0.994} Ti _{0.005} F _{1.059} OH _{0.929} O _{0.012}					
<i>Unit cell parameters</i> (Jones <i>et al.</i> , 1969)					
Estimated standard errors [in brackets] refer to the last decimal place.					
<i>a</i>	4.7408 [1] Å	Space group <i>Pbmm</i>			
<i>b</i>	10.2580 [2]	<i>Z</i> = 4			
<i>c</i>	20.8526 [4]				
<i>V</i>	1014.08 Å ³				
<i>Refractive indices, density</i> (Sahama, 1953)					
α	1.624	2 <i>V</i> = 66°			
β	1.633	Density 3.245 gm/cc.			
γ	1.653				

M(2)₆ sites. Accordingly, the concentration of Fe in the four octahedral sites was adjusted arbitrarily until the isotropic temperature factors became equal (0.5 Å²). The result was ~0.1 Fe in *M*(1) and in *M*(2)₆, 0.04 Fe in *M*(2)₅ and 0.01 Fe in *M*(3) (Ribbe and Gibbs, 1969). Subsequent site refinement using the program of Finger (1969a), gave statistically identical values for the Fe/Mg distribution: 0.09 Fe in *M*(1), 0.12 in *M*(2)₆, 0.03 in *M*(2)₅ and 0.01 in *M*(3) (see Table 3). The same Mg/Fe distribution was obtained regardless of which site was chosen to be the independent variable. Constraints on all octahedral site occupancies were Fe+Mg=1.0, with total Fe=0.4 atom.

The unweighted residual for the final isotropic refinement was 0.042. Atomic coordinates

TABLE 3. ISOTROPIC TEMPERATURE FACTORS AND CORRESPONDING Fe/Fe+Mg CONTENT [IN BRACKETS] OF OCTAHEDRAL SITES IN VARIOUS STAGES OF REFINEMENT OF THE HUMITE STRUCTURE

Site	Anion chemistry of octahedron	ORFLS Refinement		Finger Program	
		Disordered Fe	<i>B</i> constrained	Refine <i>B</i> , Fe <i>B</i> constrained	
<i>M</i> (1)	O ₆	0.2 [.05]	0.5 [.09] ₅	.44 [.09] ^a	0.39 [.09] ^a
<i>M</i> (2) ₆	O ₆	0.1 [.05]	0.5 [.10] ₅	.35 [.12]	0.39 [.11]
<i>M</i> (2) ₅	O ₅ (F, OH)	0.7 [.05]	0.5 [.04]	.33 [.03]	0.39 [.04]
<i>M</i> (3)	O ₄ (F, OH) ₂	0.9 [.05]	0.5 [.01]	.38 [.01]	0.39 [.01]

^a Estimated standard errors in Fe content range between 0.003 and 0.007.

TABLE 4. POSITIONAL PARAMETERS, ISOTROPIC TEMPERATURE FACTORS, AND R.M.S. EQUIVALENTS FOR HUMITE

(Estimated standard deviations are in parentheses and refer to the last decimal place.)

Atom	<i>x</i>	<i>y</i>	<i>z</i>	<i>B</i> (Å ²)	<i>μ</i> (Å)
<i>M</i> (1)	0.0017 (3)	0.3773 (2)	0.1767 (1)	*	
<i>M</i> (2) ₆	.5108 (5)	.1540 (2)	$\frac{1}{4}$	*	
<i>M</i> (2) ₅	.0087 (4)	.0976 (2)	.1092 (1)	*	
<i>M</i> (3)	.4925 (4)	.8665 (1)	.0278 (1)	*	
Si(1)	.0752 (5)	.9691 (2)	$\frac{1}{4}$	0.27 (5)	0.058
Si(2)	.5765 (4)	.2819 (1)	.1059 (1)	.15 (4)	.042
O(2, 3)	.7225 (8)	.2141 (4)	.1686 (2)	.49 (10)	.079
O(1, 3)	.2198 (9)	.0382 (4)	.1882 (2)	.47 (11)	.077
O(2, 4)	.7261 (8)	.2087 (4)	.0452 (2)	.35 (9)	.066
O(2, 1)	.2368 (8)	.2827 (4)	.1048 (2)	.33 (9)	.064
O(1, 2)	.2816 (13)	.3233 (6)	$\frac{1}{4}$.54 (13)	.082
O(1, 1)	.7320 (11)	.9679 (6)	$\frac{1}{4}$.57 (14)	.085
O(2, 2)	.7805 (9)	.9264 (4)	.1046 (2)	.52 (9)	.081
F, OH	.2621 (7)	.0328 (3)	.0357 (2)	.59 (8)	.086

* *B* varies with Fe/Fe+Mg concentration assigned to these octahedral sites. See Table 3.

and isotropic vibrational parameters are listed in Table 4 with the exception of the temperature factors for the octahedral cations which were given in Table 3. Interatomic distances and interbond angles for the cation coordination polyhedra are recorded in Table 5; the intercation distances and bond angles for the oxygen and (F,OH) coordination polyhedra are in Table 6.

DISCUSSION

In humite, as in olivine, norbergite, and chondrodite, the key structural unit is the serrated chain of edge-sharing *M*-octahedra running along the *c*-axis (see Fig. 1 and *cf.* Ribbe *et al.*, 1968, Fig. 3). As in all these close-packed orthosilicates, one-half the octahedral sites are filled. In humite there are four octahedral sites: *M*(1) and *M*(2)₆, like those in olivine (Birle, Gibbs, Moore, and Smith, 1968), and *M*(2)₅ and *M*(3), like those in chondrodite (Paper II). There are two distinct Si-containing tetrahedra which link the octahedral chains both within and between the close-packed anion layers: 3/28ths of the tetrahedral sites are filled.

The oxygens are coordinated to one Si and three divalent metal cations (except where trace amounts of Ti are present). The site of the monovalent anion in this particular humite is occupied by F and OH in nearly equal proportions. The (F,OH) anions are bonded to three cations in a nearly planar array (see Paper I, p. 384, Fig. 5a).

TABLE 5. Si-O, M-O AND O-O DISTANCES, O-Si-O AND O-M-O ANGLES,
AND BOND-ANGLE STRAINS IN HUMITE
(Estimated standard errors are in brackets and refer to the last decimal place.)

<i>Si(1) Tetrahedron, SiO₄</i>			<i>O(2, 3)-O(1, 1)</i>			3.116 (5)	94.4	+ 4.4
Si(1)-O(1, 1) ^A	1.628 (6)		O(1, 3)-O(2, 1)	3.152 (5)	96.3	+ 6.3		
O(1, 2)	1.642 (4)		O(1, 3)-O(2, 1)	3.341 (7)	104.0	+14.0		
O(1, 3) [2]	1.623 (6) Å		O(1, 3)-O(2, 2)	3.379 (6)	107.1	+17.1		
Mean	1.629 Å		Mean	2.971 Å	90.0°			
Angles at Si(1)* Strain**			<i>M(2)₆ Octahedron, MO₆(F, OH)₁</i>					
O(1, 3)-O(1, 2) [2]	2.553 (7) ^f	102.9°	- 6.5°	<i>M(2)-O(1, 3)^A</i>	2.022 (4) Å			
O(1, 3)-O(1, 3)	2.577 (7) ^f	105.2	- 4.2	O(2, 2) ^A	2.065 (4)			
O(1, 2)-O(1, 1)	2.742 (9)	114.0	+ 4.6°	O(2, 3)	2.191 (4)			
O(1, 3)-O(1, 1) [2]	2.744 (7)	115.2	+ 5.8	O(2, 1)	2.187 (4)			
Mean	2.652 Å	109.1°		O(2, 4)	2.208 (5)			
			F, OH			2.057 (4)		
			Mean			2.122 Å		
<i>Si(2) Tetrahedron, SiO₄</i>			<i>M(2)₆ Octahedron, MO₆(F, OH)₁</i>			Angles at <i>M(2)₆*</i>		
Si(2)-O(2, 1) ^A	1.611 (4) Å			O(2, 3)-O(2, 4)	2.573 (5) ^f	71.6°	-18.4°	
O(2, 2)	1.630 (5)			O(2, 4)-O(2, 1)	2.826 (6) ^o	80.0	-10.0	
O(2, 3)	1.634 (4)			O(2, 3)-O(2, 1)	2.865 (5) ^o	81.7	- 8.3	
O(2, 4)	1.634 (5)			O(1, 3)-O(2, 2)	2.948 (6)	92.3	+ 2.3	
Mean	1.627 Å			O(2, 3)-O(1, 3)	2.997 (5)	90.6	+ 0.6	
Angles at Si(2)* Strain**								
O(2, 3)-O(2, 2)	2.553 (6) ^f	103.0°	- 6.4°	O(1, 3)-O(2, 1)	3.053 (5)	92.9	+ 2.9	
O(2, 4)-O(2, 2)	2.554 (6) ^f	103.0	- 6.4	O(2, 4)-O(2, 2)	3.161 (5)	95.4	+ 5.4	
O(2, 3)-O(2, 4)	2.573 (5) ^f	103.9	- 5.5	O(2, 3)-O(2, 2)	3.250 (4)	99.5	+ 9.5	
O(2, 1)-O(2, 2)	2.722 (6)	114.3	+ 4.9	F, OH-O(2, 2)	2.910 (5)	89.8	- 0.2	
O(2, 4)-O(2, 1)	2.739 (5)	115.2	+ 5.8	F, OH-O(2, 1)	2.943 (5)	87.8	- 2.2	
O(2, 3)-O(2, 1)	2.750 (6)	115.9	+ 6.5	F, OH-O(2, 4)	3.123 (6)	94.1	+ 4.1	
Mean	2.648 Å	109.2°		F, OH-O(1, 3)	3.186 (5)	102.7	+12.7	
			Mean			2.986 Å	89.9°	
<i>M(1) Octahedron, MO₆</i>			<i>M(2)₆ Octahedron, MO₆</i>					
M(1)-O(2, 2)	2.075 (4) Å			<i>M(2)₆-O(1, 2)^A</i>	2.049 (6) Å			
O(1, 2)	2.098 (4)			O(2, 3) ^A [2]	2.067 (5)			
O(1, 1)	2.103 (4)			O(1, 1)	2.178 (7)			
O(2, 1)	2.106 (4)			O(1, 3) [2]	2.231 (5)			
O(1, 3)	2.127 (4)			Mean	2.137 Å			
O(2, 3)	2.141 (4)			Angles at <i>M(2)₆*</i>				
Mean	2.108 Å			Strain**				
Angles at <i>M(1)*</i>								
O(2, 3)-O(2, 2)	2.553 (6) ^f	74.5°	-15.5°	O(1, 3)-O(1, 3) ^f	2.577 (7) ^f	70.6°	-19.4°	
O(1, 3)-O(1, 2)	2.553 (6) ^f	74.4	-15.6	O(1, 3)-O(1, 1) [2]	2.842 (7) ^o	80.3	- 9.7	
O(1, 3)-O(1, 1)	2.842 (7) ^o	84.4	- 5.6	O(2, 3)-O(1, 2) [2]	2.917 (6)	90.3	+ 0.3	
O(1, 2)-O(1, 1)	2.851 (8) ^o	85.5	- 4.5	O(1, 3)-O(2, 3) [2]	3.018 (8)	89.1	-10.9	
O(2, 1)-O(2, 2)	2.862 (5) ^o	86.4	- 3.6	O(2, 3)-O(1, 1) [2]	3.044 (5)	91.6	+ 1.6	
O(2, 3)-O(2, 1)	2.865 (5) ^o	84.8	- 5.2	O(1, 3)-O(1, 2) [2]	3.210 (6)	97.1	+ 7.1	
O(2, 1)-O(1, 2)	3.063 (5)	93.5	+ 3.5	O(2, 3)-O(2, 3) ^f	3.395 (8)	110.5	+20.5	
O(1, 1)-O(2, 2)	3.070 (4)	94.6	+ 4.6	Mean	3.003 Å	89.8°		

TABLE 5.—*Continued*

<i>M</i> (3) Octahedron, <i>MO</i> ₄ (<i>F</i> , <i>OH</i>) ₂				O(2, 4)–O(2, 1)	2.826 (6) ^o	83.3	– 6.7
<i>M</i> (3)–O(2, 4) ^A	1.996 (4) Å			O(2, 1)–O(2, 2)	2.862 (5) ^o	83.1	– 1.9
O(2, 1)	2.122 (4)			F, OH–F, OH'	2.786 (7) ^o	86.2	– 3.8
O(2, 4)'	2.129 (4)			F, OH–O(2, 4)	2.852 (6)	89.8	– 0.2
O(2, 2)	2.193 (4)			F, OH–O(2, 1)	2.943 (5)	90.2	+ 0.2
F, OH	2.032 (4)			F, OH'–O(2, 2)	2.963 (5)	88.7	– 1.3
F, OH'	2.043 (4)			F, OH'–O(2, 4)'	2.998 (4)	96.2	+ 6.2
Mean	2.086 Å			F, OH'–O(2, 2)	3.049 (5)	92.3	+ 2.3
		Angles		F, OH'–O(2, 4)	3.148 (4)	97.9	+ 7.9
		at	Strain**	O(2, 1)–O(2, 4)'	3.130 (5)	98.9	+ 8.9
		<i>M</i> (3)*		O(2, 4)–O(2, 4)'	3.145 (6)	99.3	+ 9.3
				Mean	2.938 Å	89.9 ^o	
O(2, 4)–O(2, 2)	2.554 (6) ^t	72.4 ^o	–17.6 ^o				

* The estimated standard error in all bond angles is 0.1°

** Strain = observed minus ideal

^t edge shared between tetrahedron and octahedron

^o edge shared between two octahedra

Oxygen Coordination

It would be duplicative to discuss at length the details of the coordination polyhedra in humite, because the observed bond angle strains, taken as a measure of the distortion of the structure from an ideal hcp anion array, are very similar to those discussed in Papers I and II for norbergite and chondrodite. The intercation distances and cation-oxygen-cation bond angles with their corresponding ideal angles and bond angle strains (observed minus ideal) are recorded in Table 6.

Emerging from a consideration of the three oxygens in norbergite, the four in chondrodite, and the seven in humite is an average picture of the two types of oxygen coordination polyhedra, shown in Figure 2. Both the M_A -O and Si_A -O bonds are somewhat shorter than the respective Mg-O and Si-O bonds (subscripts *A* and *B* signify the apical and basal positions in the oxygen coordination polyhedron). This arises from the fact that the apical-basal cation pairs are in adjacent corner-sharing cation polyhedra whereas the basal-basal pairs are in edge-sharing polyhedra. The angle strains at oxygen are related to the intercation distances (Fig. 3), and because of repulsion across shared edges, the strains are always positive for the M_B -O- Si_B and M_B -O- M_B angles and negative for the M_A -O- M_B bond angles. The M_B -O- M_B bond angle strains are on the average one degree greater when Si is in the basal array (solid dots) than when Si is in the apical position (crosses), reflecting the greater repulsion between Si and the two *M* cations in the basal array.

SiO_4 Tetrahedra

Steric details of the two SiO_4 tetrahedra are given in Table 5 and Figure 4. The $Si(2)O_4$ tetrahedron (symmetry C_1) is very similar to the

TABLE 6. DETAILS OF ANION COORDINATION IN HUMITE

	Inter-cation distance	Angle at oxygen	Ideal angle	Strain
O(2, 3)				
$M(2)_{6,A}-Si(2)_B$	3.293 Å	125.3°	125.3°	0.0°
$-M(2)_{5,B}$	3.812	127.0	131.8	-4.8
$-M(1)_B$	3.605	117.9	131.8	-13.9
$M(2)_{5,B}-M(1)_B$	3.197	95.1	90.0	+5.4
$-Si(2)_B$	2.789	92.4	79.5	+12.9
$M(1)_B-Si(2)_B$	2.683	89.6	79.5	+10.1
O(1, 3)				
$M(2)_{5,A}-Si(1)_B$	3.234 Å	124.7°	125.3°	-0.6°
$-M(2)_{6,B}$	3.824	128.1	131.8	-3.7
$-M(1)_B$	3.533	116.7	131.8	-15.1
$M(2)_{6,B}-M(1)_B$	3.224	95.4	90.0	+5.4
$-Si(1)_B$	2.804	92.0	79.5	+12.5
$M(1)_B-Si(1)_B$	2.691	90.7	79.5	+11.2
O(2, 4)				
$M(3)_A-Si(2)_B$	3.193 Å	122.9°	125.3°	-2.6
$-M(2)_{5,B}$	3.733	125.2	131.8	-6.6
$-M(3)_B$	3.559	119.3	131.8	-12.5
$M(2)_{5,B}-M(3)_B$	3.239	96.6	90.0	+6.6
$-Si(2)_B$	2.789	91.9	79.5	+12.4
$M(3)_B-Si(2)_B$	2.754	93.2	79.5	+13.7
O(2, 1)				
$Si(2)_A-M(2)_{5,B}$	3.290 Å	119.3°	125.3°	-6.0°
$-M(3)_B$	3.269	121.7	125.3	-3.6
$-M(1)_B$	3.251	121.4	125.3	-3.9
$M(2)_{5,B}-M(3)_B$	3.239	97.5	90.0	+7.5
$-M(1)_B$	3.197	96.2	90.0	+6.2
$M(3)_B-M(1)_B$	3.109	94.7	90.0	+4.7
O(1, 2)				
$M(2)_{6,A}-Si(1)_B$	3.258 Å	123.6°	125.3°	-1.7°
$-M(1)_B$	[2] 3.662	124.0	131.8	-7.8
$M(1)_B-M(1)_B$	3.055	93.5	90.0	+3.5
$-Si(1)_B$	[2] 2.691	91.2	79.5	+11.7
O(1, 1)				
$Si(1)_A-M(2)_{5,B}$	3.280 Å	118.3°	125.3°	-7.0°
$-M(1)_B$	[2] 3.271	122.0	125.3	-3.3
$M(1)_B-M(2)_{6,B}$	[2] 3.224	97.7	90.0	+7.7
$-M(1)_B$	3.055	93.2	90.0	+3.2
O(2, 2)				
$M(2)_{5,A}-Si(2)_B$	3.264 Å	123.7°	125.3°	-1.6°
$-M(3)_B$	3.807	126.7	131.8	-5.1
$-M(1)_B$	3.598	120.7	131.8	-11.1
$M(3)_B-M(1)_B$	3.109	93.5	90.0	+3.5
$-Si(2)_B$	2.754	90.9	79.5	+11.4
$M(1)_B-Si(2)_B$	2.683	92.0	79.5	+12.5
F, OH				
$M(2)_5-M(3)$	3.710 Å	130.3°	131.8°	-1.5°
$-M(3)'$	3.726	130.7	131.8	-1.1
$M(3)-M(3)'$	2.975	93.7	90.0	+3.7

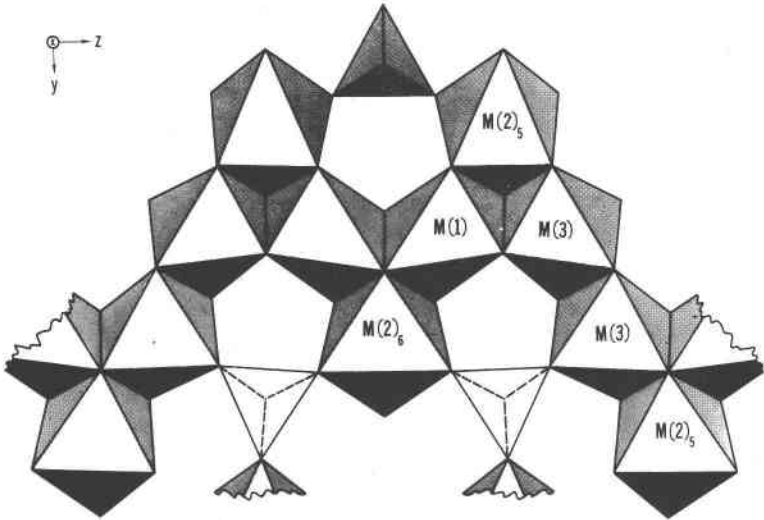


FIG. 1. Serrated chain of edge-sharing M -octahedra in humite in the plane of the h.c.p. anions.

tetrahedra in norbergite and chondrodite. The $\text{Si}(2)$ -O bonds to the oxygens defining edges shared with the $M(1)$, $M(2)_B$, and $M(3)$ octahedra are longer (1.630–1.634 Å) than the $\text{Si}(2)_A$ -O distance (1.611 Å).

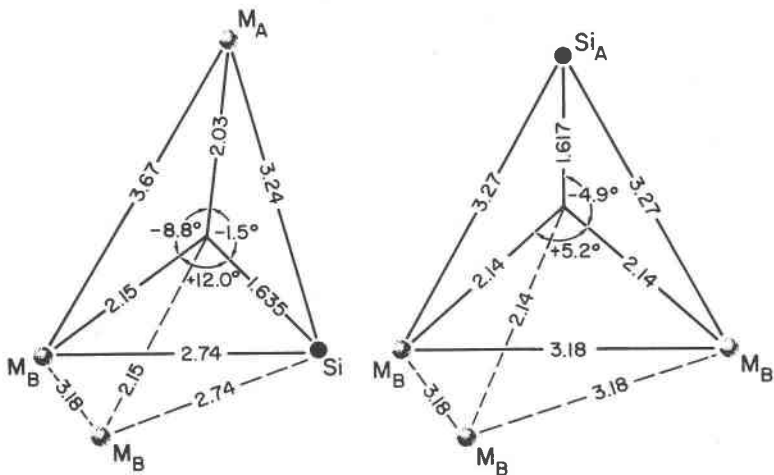


FIG. 2. Composite oxygen coordination diagrams using means of the interatomic distances and bond-angle strains from ten oxygen atoms in norbergite, chondrodite, and humite for the diagram on the left and four for the one on the right. Subscripts A and B signify the apical and basal positions in the coordination tetrahedron.

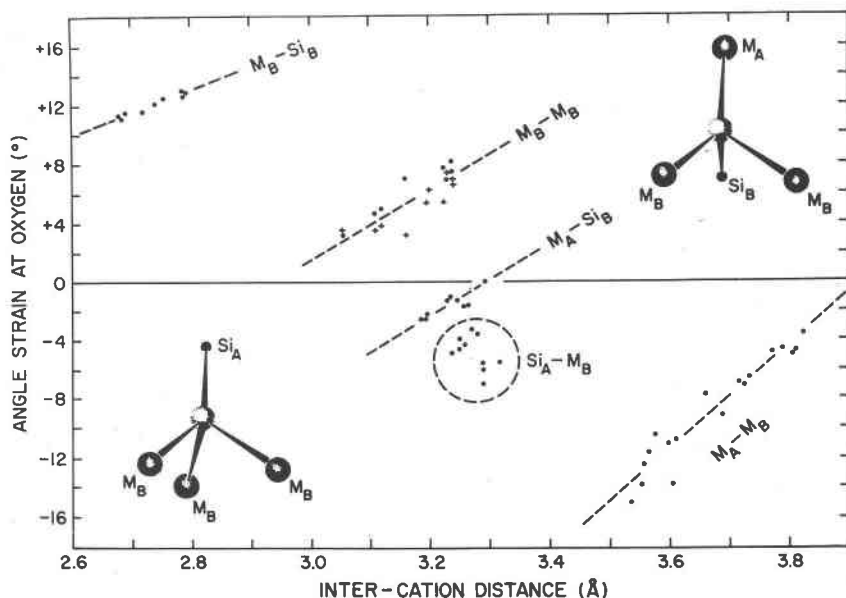


FIG. 3. The relation of angle strains (observed minus ideal for h.c.p.) at oxygen as a function of inter-cation distance using data from norbergite, chondrodite, and humite. The largest positive strains are associated with the large $M_B^{2+}-Si_B^+$ repulsion across shared polyhedral edges. The M_B-O-M_B strains are on the average one degree greater when Si is in the basal array (solid dots) than when Si is in the apical position (crosses).

In the humite minerals examined thus far only the $Si(1)O_4$ tetrahedron (symmetry C_s) in humite is completely surrounded by three edge shared and three corner shared MO_6 octahedra; the SiO_4 tetrahedron in norbergite is surrounded by six MO_4F_2 octahedra. By comparison, SiO_4 in chondrodite and $Si(2)O_4$ in humite each share an edge and a corner with $M(1)$, $M(2)$, and $M(3)$ octahedra, and in fact the $Si(2)O_4$ tetrahedron in humite is a slightly smaller version of the SiO_4 tetrahedron in chondrodite.

An examination of the mean of the two Si-O bond lengths opposite shared edges in olivine (Fig. 5) shows that they decrease with increasing M-Si distance (Brown and Gibbs, 1971). The M-Si distance is dependent on the radius of the M cation and the data represent two populations, one associated with the smaller $M(1)$ site (solid circles) and the other with the larger $M(2)_6$ sites (heavy crosses). Assuming that the average bond order of an Si-O bond within a tetrahedron is essentially constant ($n=1.5$), it follows that if one bond lengthens, then one or more must shorten to preserve the average bond order (see discussion in Mitchell,

forsterite (Fo) and humite (Hu), the mean Si-O bond length to the shared edge is ~ 0.015 Å shorter in humite. Geometrically this can be accomplished by a thinning of the octahedral layer which widens the M -O-Si angles across the shared edge, rotating the Si toward the shared edge, thereby decreasing the mean Si-O bond length. The thinning of the octahedral layer is due to the coupled substitution of 4(O) by 4(F,OH) and a silicon by a tetrahedral void (Ribbe *et al.* 1968). The Si-O bonds opposite edges shared with $M(2)_5$, $M(2)_4$, and $M(3)$ octahedra in the humite minerals are also shorter, but the mechanism is complicated by the effects of shortened M -(F,OH) bonds in these octahedra.

M Octahedra and the Effective Radii of Two- and Three-coordinated OH⁻.

Comparisons of overall mean M -O and M -(F,OH) bond length and O-O, (F,OH)-O and (F,OH)-(F,OH) shared and unshared octahedral edges for humite, chondrodite, and norbergite are given in Table 7. Plots of the mean interatomic distances associated with the (F,OH) site as

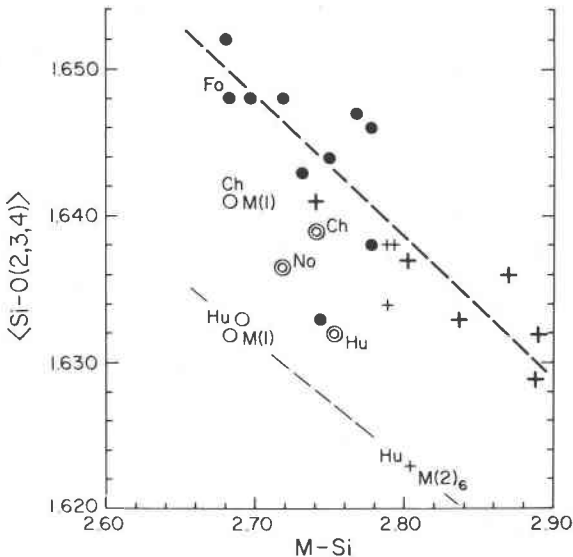


FIG. 5. The means of the two Si-O bond lengths opposite edges shared between octahedra and tetrahedra *versus* the M -Si distance across the shared edges (in Ångströms) for non-calcium olivines ($M(1)$ cations, solid dots; $M(2)$ cations, heavy crosses), norbergite (No), chondrodite (Ch), and humite (Hu). Note that the forsterite (Fo), chondrodite, and humite $M(1)$ -Si distances are nearly identical. See text for comments. The $M(3)$ cation-No, Ch, and Hu are shown as double circles; the $M(2)_5$ and $M(2)_4$ cations are shown as light crosses. Olivine data from Brown (1970).

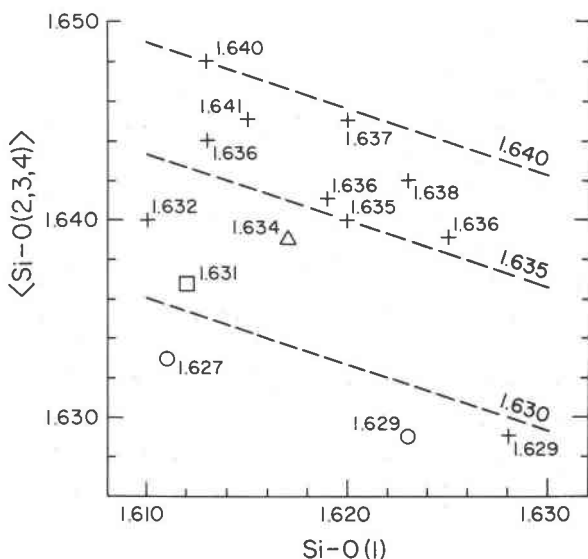


FIG. 6. Mean Si-O bond lengths in Ångstroms to shared edges (abscissa) versus the Si-O bond length to apical O(1) for olivines (crosses), norbergite (square), chondrodite (triangle), and humite (circles). The dashed contour lines have a slope of $-1/3$. Data for the noncalcium olivines from Brown (1970).

a function of the fluorine content (Fig. 7) show that the effective radius of OH is 0.04 \AA larger than F. This is in good agreement with values obtained from M -(F,OH) bond lengths in tremolite (Papike, Ross, and Clark, 1969) and protoamphibole (Gibbs, 1969) and from volume considerations in topaz (Ribbe and Rosenberg, in press), where (F,OH) is two-coordinated. Thus the proposed radii for three- and two-coordinated OH are 1.34 and 1.32 , Å, respectively, based on Shannon and Prewitt's (1969) fluorine radii.

The $M(2)$ octahedra of the humite minerals and forsterite are ideally suited for comparison of the effects of $(F+OH):(F+OH+O)$ on the mean M -(O,F,OH) distance because $M(2)_4$ of norbergite, $M(2)_6$ of humite and chondrodite, and $M(2)_6$ of humite and forsterite each share two O-O edges with other octahedra and one O-O edge with a tetrahedron. Thus Figure 8 shows that anion ligancy has a first order effect on the size. At this scale, however, the effect of the larger Fe^{2+} ion ($r=0.77 \text{ \AA}$) replacing Mg ($r=0.72 \text{ \AA}$) in an octahedral site is significant, and the relationship between mean M -(O,F,OH) bond length and total $(F+OH)$ replacing O is linear when corrections are made for Fe^{2+} content (see Table 7).

TABLE 7. MEAN INTERATOMIC DISTANCES FOR THREE HUMITE MINERALS

		Humite ($F_{1.06}OH_{0.93}$)	Chondrodite ($F_{1.27}OH_{0.73}$)	Norbergite ($F_{1.81}OH_{0.17}$)
	O-O	3.117	3.135	3.138
Unshared octahedral edges	F, OH-O	3.012	3.003	2.991
	F-F	—	—	2.915
Edges shared between octahedral	O-O	2.848	2.831	2.826
	F, OH-F, OH	2.786	2.764	2.689
Unshared tetrahedral edges	O-O	2.740	2.750	2.740
Edges shared between tetrahedra and octahedra	O-O	2.561	2.568	2.568
Octahedral bond lengths	M-O	2.123	2.114	2.124
	M-F, OH	2.044	2.034	2.012
Tetrahedral bond lengths	Si-O	1.628	1.634	1.631

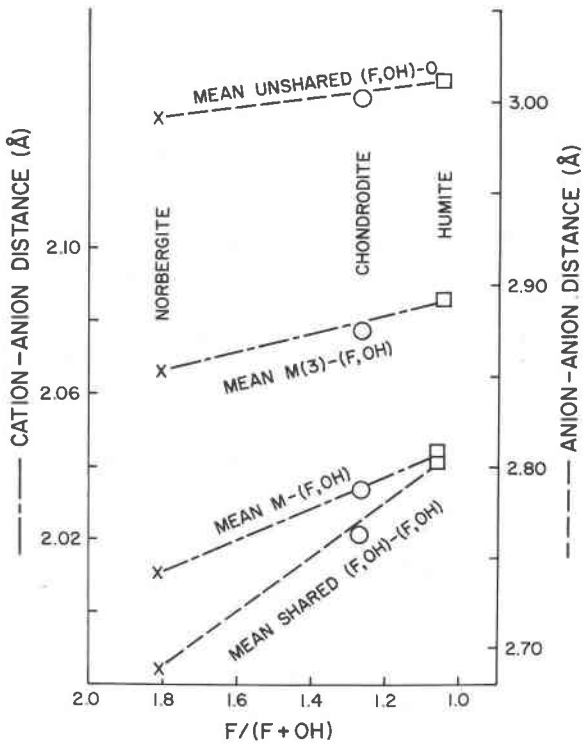


FIG. 7. Plots of the mean interatomic distances involving the monovalent anion in norbergite, chondrodite, and humite as a function of fluorine content (2 minus $F=OH$ content). The dashed lines are referred to the right scale and the dash-dot lines to the left. The latter were used in deducing the effective radius of three-coordinated OH^- (see text).

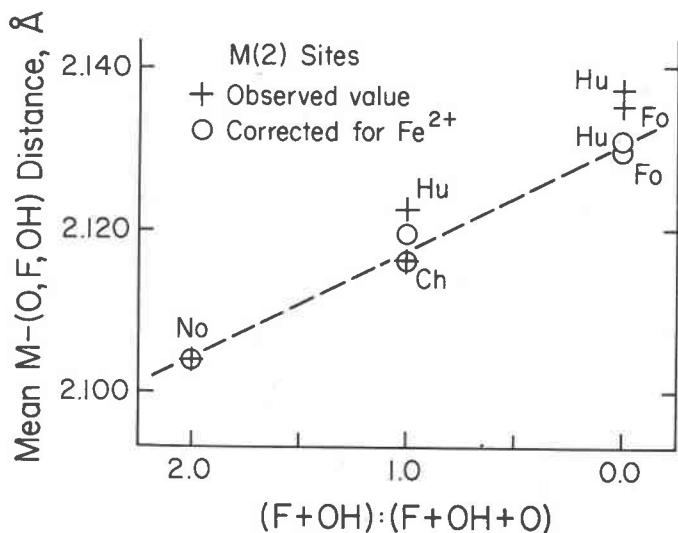


FIG. 8. Mean $M-(O,F,OH)$ distances as a function of $(F+OH)$ content in the norbergite (No) $M(2)_4$ octahedron, the chondrodite (Ch) and humite (Hu) $M(2)_6$ octahedra, and the humite and forsterite (Fo) $M(2)_6$ octahedra. Open circles represent the values adjusted for Fe^{2+} content (see Table 8).

Mg/Fe Ordering in Humite and Other Silicates

Burns (1970) has examined the absorption spectra of a large number of ferromagnesian silicates and has concluded from crystal field theory and size criteria that Fe^{2+} should prefer the larger and more distorted polyhedral sites. He predicts the following site preferences for Fe^{2+} : $M(2) > M(1)$ in orthopyroxene and olivine, $M(4) > M(2) > M(1), M(3)$ for the cummingtonite-grunerite series and the anthophyllite series, and $M(2) > M(1), M(3)$ in actinolite. The $M(2)$ sites in orthopyroxene are larger and more distorted than the $M(1)$ sites, and as predicted Fe^{2+} is enriched in $M(2)$ (Ghose, 1965; Virgo and Hafner, 1969). In Mg/Fe amphibole Fe^{2+} is also enriched in the largest, most distorted $M(4)$ site which is very similar to $M(2)$ in orthopyroxene. However, among the other three sites in Mg/Fe- as well as Ca- and Na-amphiboles, Fe^{2+} , is enriched in the $M(3)O_4(OH,F)_2$ and the $M(1)O_4(OH,F)_2$ octahedra relative to the $M(2)O_6$ octahedron as follows:

Cummingtonite	$M(3) = M(1) > M(2)$	(Ghose, 1961; Fisher, 1966)
Mn-cummingtonite	$M(3) > M(1) \geq M(2)$	(Papike <i>et al.</i> , 1969)
Grunerite	$M(3) > M(1) > M(2)$	(Finger, 1969 b)
Glaucofane	$M(3) > M(1) > M(2)$	(Papike and Clark, 1968)
Actinolite	$M(1) \geq M(3) > M(2)$	(Mitchell <i>et al.</i> , 1971)

These distributions do not agree with Burns' prediction that Fe^{2+} prefers the $M(2)$ octahedron which, on the basis of range of M -O bond lengths, he considered to be more distorted than $M(1)$ or $M(3)$. In fact it can be shown using the quadratic elongation parameter of Robinson, Gibbs, and Ribbe (1971) that the $M(3)$ octahedra are consistently more distorted than both $M(1)$ and $M(2)$. However, neither size (*cf.* mean M -O distances in tremolite; Papike *et al.*, 1969) nor distortion criteria explain in detail the observed Fe^{2+} distribution.

Furthermore, it is difficult to rationalize these distributions in amphiboles in terms of the Mg/Fe distributions observed in humite and chondrodite where Fe^{2+} is concentrated into those sites with six oxygen ligands [in humite $M(1)=0.09$ Fe; $M(2)_6=0.12$ Fe; in chondrodite $M(1)=0.05$ Fe], but avoids the sites with (F,OH) ligands [in humite $M(2)_5=0.03$ Fe; $M(3)=0.01$ Fe; in chondrodite $M(1)=M(3)=0.00$ Fe]. See Figure 9. In these humite minerals the Mg/Fe distribution is not dependent on the sizes of the octahedra or their distortions as measured by either of two criteria, the range of bond angle strains (R_s =largest minus smallest octahedra angle] or the range of M -(O,F,OH) bond lengths (see Table 8). However, there does appear to be a correlation with both anion liganacy and octahedral distortion as measured by the

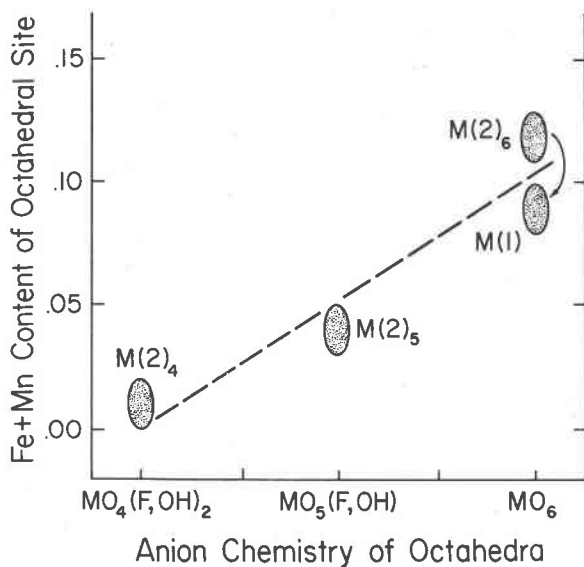


FIG. 9. (Fe+Mn) content of the octahedral site as a function of anion chemistry in humite. If the large $M(2)_6$ site is assumed to contain most of the small amount of Mn in this humite, and the curved arrow indicates that the Fe^{2+} content would then be about the same as the $M(1)$ site.

TABLE 8. DETAILS OF LIGANCY, Fe/Mg DISTRIBUTION AND OCTAHEDRAL GEOMETRY FOR THE HUMITE MINERALS AND FORSTERITE

Site	Ligancy	Fe/Fe+Mg	Range of bond-angle strains, R_s	Range of bond lengths	Mean $M-(O, F, OH)$	Quadratic elongation
Humite						
$M(1)$	O_6	.09	32.6°	.066 Å	2.108 Å	1.0293
$M(2)_6$	O_6	.12	39.9°	.182	2.137	1.0291
$M(2)_5$	$O_3F_{0.53}OH_{0.47}$.03	31.1°	.186	2.122	1.0223
$M(3)$	$O_{4.01}F_{1.06}OH_{0.93}$.01	26.9°	.197	2.086	1.0190
Chondrodite (Paper II)						
$M(1)$	O_6	.05	29.8°	.029	2.108	1.0279
$M(2)_5$	$O_3F_{0.64}OH_{0.36}$.00	30.0°	.177	2.116	1.0244
$M(3)$	$O_4F_{1.27}OH_{0.73}$.00	25.4°	.188	2.078	1.0179
Norbergite (Paper I)						
$M(2)_4$	$O_{4.02}F_{1.81}OH_{0.17}$.00	26.7°	.198	2.104	1.0236
$M(3)$	$C_{4.02}F_{1.81}OH_{0.17}$.00	24.2°	.189	2.068	1.0185
Forsterite (Brown, 1970)						
$M(1)$	O_6	.10	30.6°	.066	2.101	1.0280
$M(2)_6$	O_6	.10	39.3°	.164	2.135	1.0273

quadratic elongation. Table 8 shows that $M(1)O_6$ and $M(2)O_6$ in humite and $M(1)O_6$ in chondrodite are more distorted and contain more Fe^{2+} than the $M(2)O_5(F,OH)$ and $M(3)O_4(F,OH)_2$ octahedra.

If the distribution of Fe^{2+} in Mg/Fe silicates is related to the splitting of the ligand field, Dq , then it is possible to rationalize the preference of Fe^{2+} for those octahedral sites ligated only by oxygen on the basis of the Fajans-Tsuchida spectrochemical series. For a given metal and stereochemistry Dq increases with ligand in the following order: . . . $Cl^- < S^{2-} < F^- < OH^- < O^{2-} < H_2O$. . . (Lever, 1969). This is another way of stating that O^{2-} is more polarizable than OH^- and F^- and forms a stronger σ -covalent bond with Fe^{2+} .

Thus in humite both anion ligancy and octahedral distortion may enhance the ligand field stabilization energy of Fe^{2+} in the $M(1)O_6$ and $M(2)O_6$ octahedra relative to $M(2)O_5(F,OH)$ and $M(3)O_4(F,OH)_2$. However, in the amphiboles Fe^{2+} is less concentrated in $M(2)O_6$, preferring the more irregular $M(3)O_4(OH,F)_2$ and $M(1)O_4(OH,F)_2$ octahedra. If anion ligancy does contribute significantly to the ligand field stabilization energy of Fe^{2+} , it would appear that certain of the oxygens coordinating the $M(2)$ cation in amphiboles may be less polarizable than the OH and F ligands of $M(3)$ and $M(1)$ cations. This interpretation is plausible since the $M(2)$ cation is bonded to two charge-balanced O(1)

atoms, two O(2) atoms, which are slightly electrostatically undersaturated (~ 1.9), and two O(4) atoms which are highly undersaturated (1.6–1.7). By contrast the $M(3)$ cation is bonded to four charge-balanced O(1) atoms, and two charge-balanced O(1) atoms and two charge-balanced (OH,F) atoms, and the $M(1)$ cation is bonded to two O(1), two (OH,F), and two slightly under-saturated O(2) atoms.

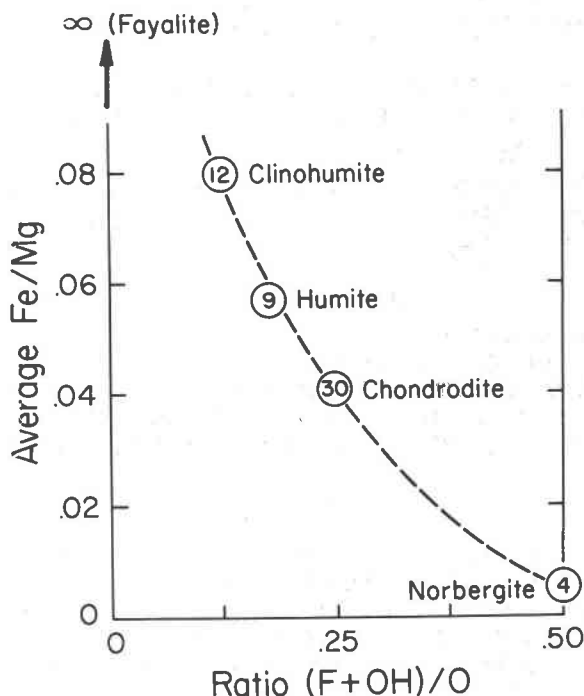


FIG. 10 The average Fe/Mg ratio plotted against (F+OH)/O for 55 humite minerals (microprobe analyses by Jones, 1968). Numbers of analyses for each mineral are encircled. The less (F,OH)-rich humite minerals contain more Fe^{2+} , and in olivine, which has no (F,OH), Fe^{2+} substitution for Mg is unlimited.

In conclusion, the Mg/Fe distribution in humite and chondrodite cannot be rationalized in terms of ionic size. In these close-packed orthosilicates all of the anions are charge-balanced, and Fe^{2+} prefers the more distorted sites and those with the more polarizable ligands. In Mg-Fe olivines where all the ligands are charge-balanced oxygens, site refinements indicate highly disordered configurations (Brown, 1970); however, two recent site refinements by Finger (1970) indicate a slight ordering of Fe^{2+} into the $M(1)$ site. Although $M(1)$ is significantly

smaller than $M(2)$, it is also slightly more distorted than $M(2)$ as measured by the quadratic elongation criterion (Robinson *et al.*, 1971).

Although the site refinement (Table 8) indicates that the larger $M(2)_6$ site in humite is slightly more Fe^{2+} -rich than $M(1)$, this difference can be attributed to preference of Mn^{2+} (previously combined with Fe in the scattering curve) for the $M(2)_6$ site. This is consistent with the results of a refinement of $\text{Fe}_{1.02}\text{Mn}_{0.93}\text{Mg}_{0.05}\text{SiO}_4$ by Brown and Gibbs (1971) which showed twice as much Mn as Fe in the $M(2)_6$ site as in the $M(1)$ site.

The importance of F and OH in the partitioning of Fe^{2+} amongst the minerals of the humite series is shown in Figure 10 where norbergite, in which all octahedra are coordinated by two F ligands, contains virtually no Fe^{2+} . The less (F,OH)-rich members of the series contain progressively more Fe^{2+} ; the olivine series, with no (F,OH) ligands, has unlimited substitution.

ACKNOWLEDGEMENTS

The authors are grateful to Mr. H. E. Rowlett, Jr., now at Columbia University, for collecting the intensity data and to the National Science Foundation for Grants GA-1133 and GA-12702. Professor L. Taylor of the Chemistry Department at V.P.I. and S. U. is thanked for his contribution to our understanding of ligand field theory. Prof. Stephan Hafner of the University of Chicago reviewed the manuscript and offered many helpful suggestions.

REFERENCES

- BIRLE, J. D., G. V. GIBBS, P. B. MOORE, AND J. V. SMITH (1968) Crystal structures of natural olivines. *Amer. Mineral.* **53**, 807-824.
- BORNEMAN-STARYNKEVICH, I. D., AND V. S. MYASNIKOV (1950) On isomorphous replacements in clinohumite. *Doklady Acad. Sci., U.S.S.R.* **71**, 137-144.
- BRAGG, W. L., AND J. WEST (1927) The structure of certain silicates. *Proc. Roy. Soc.* **114**, 450-453.
- BROWN, G. E. (1970) *Crystal chemistry of the olivines*. Ph.D. thesis, Virginia Polytechnic Institute, Blacksburg, Virginia.
- , AND G. V. GIBBS (in press) Crystal chemistry of the olivines. *Amer. Mineral.*
- BROWN, G. E., AND G. V. GIBBS (1971) Crystal chemistry of the olivines. *Amer. Mineral.* **56**,
- BURNS, R. G. (1970) *Mineralogical Applications of Crystal Field Theory*. Cambridge University Press, Cambridge, England.
- BUSING, W. R., K. O. MARTIN, AND H. A. LEVY (1962) ORFLS, a Fortran crystallographic least-squares program. Oak Ridge National Lab. [*U. S. Clearinghouse Fed. Sci. Tech. Info.*] Doc. **ORNL-TM-305**.
- FINGER, L. W. (1969a) Determination of cation distributions by least-squares refinement of single-crystal X-ray data. *Carnegie Inst. Wash. Year Book* **67**, 216-217.
- (1969b) Crystal structure and cation distribution of a grunerite. *Mineral. Soc. Amer. Spec. Pap.* **2**, 95-100.
- (1970) Cation ordering in olivines. *Carnegie Inst. Wash. Year Book* **69**, 302-305

- FISCHER, K. F. (1966) A further refinement of the crystal structure of cummingtonite, $(\text{Mg,Fe})_7(\text{Si}_4\text{O}_{11})_2(\text{OH})_2$. *Amer Mineral.* **51**, 814–818.
- GHOSE, S. (1961) The crystal structure of a cummingtonite. *Acta Crystallogr.* **14**, 622–627.
- (1965) Mg^{2+} - Fe^{2+} order in an orthopyroxene $\text{Mg}_{0.93}\text{Fe}_{1.07}\text{Si}_2\text{O}_6$. *Z. Kristallogr.* **122**, 81–99.
- GIBBS, G. V. (1969) Crystal structure of protoamphibole. *Mineral. Soc. Amer. Spec. Pap.* **2**, 101–109.
- , AND P. H. RIBBE (1969) The crystal structures of the humite minerals: I. Norbergite. *Amer. Mineral.* **54**, 376–390.
- , ———, AND C. W. ANDERSON (1970) The crystal structures of the humite minerals. II. Chondrodite. *Amer. Mineral.* **55**, 1182–1194.
- JONES, N. W. (1968) *Crystal Chemistry of the Humite Minerals*. Ph.D. dissertation, Virginia Polytechnic Institute, Blacksburg, Virginia.
- (1969) Crystallographic nomenclature and twinning in the humite minerals. *Amer. Mineral.* **54**, 309–313.
- , P. H. RIBBE, AND G. V. GIBBS (1969) Crystal chemistry of the humite minerals. *Amer. Mineral.* **54**, 391–411.
- LEVER, A. B. P. (1969) *Inorganic Electronic Spectroscopy*. Elsevier Publishing Co., New York, N. Y., pp. 203–207.
- MITCHELL, J. T., F. D. BLOSSE, AND G. V. GIBBS (1971) Examination of the actinolite structure and four other $C2/m$ amphiboles in terms of doubling bonding. *Z. Kristallogr., Laves Festband* (in press).
- PAPIKE, J. J., AND J. R. CLARK (1968) The crystal structure and cation distribution of glaucophane. *Amer. Mineral.* **53**, 1156–1173.
- , M. R. ROSS, AND J. R. CLARK (1968) Crystal-chemical characterization of clinopyroxenes based on five new structure refinements. *Mineral. Soc. Amer. Spec. Pap.* **2**, 117–136.
- RANKAMA, K. (1938) On the mineralogy of some members of the humite group found in Finland. *Bull. Comm. Geol. Finlande* **123**, 81–93.
- RIBBE, P. H., AND G. V. GIBBS (1969) Mg/Fe ordering in humite, $\text{Mg}_{6.6}\text{Fe}_{0.4}\text{Si}_3\text{O}_{12}\text{F}(\text{OH})$ [abstr.] *Geol. Soc. Amer. Ann. Meet., Atlantic City*, p. 188.
- , ———, AND N. W. JONES (1968) Cation and anion substitutions in the humite minerals. *Mineral. Mag.* **37**, 966–975.
- , AND P. E. ROSENBERG (in press) Optical and X-ray determinative methods for fluorine in topaz. *Amer. Mineral.*
- ROBINSON, K., G. V. GIBBS, AND P. H. RIBBE (1971) Quadratic elongation: a quantitative measure of distortion in coordination polyhedra. *Science* (in press).
- SAHAMA, TH. G. (1953) Mineralogy of the humite group. *Ann. Acad. Sci. Fenn. A* **111**, *Geol. Geogr.* **33**, 1–50.
- SHANNON, R. D., AND C. T. PREWITT (1969) Effective ionic radii in oxides and fluoride. *Acta Crystallogr.* **B25**, 925–946.
- TAYLOR, W. H., AND J. WEST (1928) The crystal structure of the chondrodite series. *Proc. Roy. Soc.* **117**, 517–532.
- (1929) The structure of norbergite. *Z. Kristallogr.* **70**, 461–474.
- VIRGO, D., AND S. HAFNER (1969) Fe^{2+} -Mg order-disorder in heated orthopyroxenes. *Mineral. Soc. Amer. Spec. Pap.* **2**, 67–81.

Manuscript received, August 30, 1970; accepted for publication, February 8, 1971.